Mechanics and Mechanical Engineering
Vol. 22, No. 4 (2018) 895–907

https://doi.org/10.2478/mme-2018-0070

Effect of Printing Parameters on the Mechanical Properties of Parts Fabricated with Open-Source 3D Printers in PLA by Fused Deposition Modeling

M. Ouhsti, B. El Haddadi
Laboratory of Sustainable Development,Department of Physics, Faculty of Science and Technology, Sultan Moulay Slimane University, Mghila, B.P : 523, Beni Mellal, Morocco

S. Belhouideg
Team of Applied Physics and New Technologies, Department of Physics, Polydisciplinary Faculty, Sultan Moulay Slimane University, Beni Mellal, Morocco, Mghila, B.P.: 592, Beni Mellal, Morocco, soufianebelhouideg@gmail.com

Received (19 March 2018)
Revised (15 November 2018)
Accepted (20 November 2018)

3D polymer-based printers have become easily accessible to the public. Usually, the technology used by these 3D printers is Fused Deposition Modelling (FDM). The majority of these 3D printers mainly use acrylonitrile butadiene styrene (ABS) and polylactic acid (PLA) to fabricate 3D objects. In order for the printed parts to be useful for specific applications, the mechanical properties of the printed parts must be known. The aim of this study is to determine the tensile strength and elastic modulus of printed materials in polylactic acid (PLA) according to three important printing parameters such as deposition angle, extruder temperature and printing speed. The central composite design (CCD) was used to reduce the number of tensile test experiments. The obtained results show that the mechanical properties of printed parts depend on printing parameters. Empirical models relating response and process parameters are developed. The analysis of variance (ANOVA) was used to test the validity of models relating response and printing parameters. The optimal printing parameters are determined for the desired mechanical properties.

Keywords: 3D printing; Fused deposition modelling; Design of experiments; PLA; Tensile test.

1. Introduction

The additive manufacturing (AM) or 3D printing is a new technology used to produce three-dimensional pieces. The new object was created adding the material layer by layer. This technology has a major impact on innovation, design and manufacturing practices in companies. It is allow to fabricate functional pieces having complex geometrical shape in reasonable time period, without incurring any further costs due of absence of tooling [1]. The additive manufacturing (AM) is used in several fields such as civil engineering, aeronautic industry and clinical medicine (e.g., dental/orthopedic surgery) [2]. Additive manufacturing technologies include fused deposition modeling (FDM), stereolithography (SLA), Inkjet printing, and selective laser sintering (SLS) [3–5]. A systematic review of additive manufacturing technology was presented by Ford and Despeisse [6]. It is reveals that the properties of 3D printed object depend on several printing parameters and can be significantly improved with proper adjustment. However, many difficulties appear in the additive manufacturing such as high cost of the commercial machines, material restrictions and study process parameters.

Recently an open source model, the RepRap (Replication Rapid prototype), has been developed. The most RepRap machines are based on the FDM technology. Also, this model allowed to greatly expand the potential user base of rapid prototypers. In the last years, open-source 3D printers are increasingly used [7]. These machines are already used for art, toys, tools, household items and to make high-value scientific instruments [8]. In addition, other versions of at-home desktop 3D printers are also selling rapidly. While open source models have limitations compared to commercial processes [9], they are capable of creating highly accurate parts with positioning accuracy of 0.1 mm [7].

A range of materials such as polymers, ceramics or metals can be used by the 3D printers. The polylactic acid (PLA) is a popular and important biodegradable polymer usually used by FDM technology. PLA is polyester obtained from a monomer (lactic acid) derived from renewable resources such as corn sugar, potato and sugar cane [10]. A ring-opening poly-reaction of this monomer is used to manufacture the PLA. The PLA was discovered by Carothers in 1932 [11, 12]. It is the most polymer used in several field for the past five decades. The PLA has appreciable mechanical and thermal properties. PLA is used in several filed such as medicine and tissue engineering [13,14] and manufacturing of everyday items, e.g., food packaging, flatware or bottles [15–17]. It is used to make bone screws, bone plates and pin structures [18]. Also, the PLA can be used to replace metal implants in the near future [19]. The PLA is widely used in biomedical applications [20, 21]. The mechanical properties of neat PLA was evaluated by Olivieri et al. [22] according to ASTM D882 method. The Young's modulus measured by tensile tests is equal to 2630±200 MPa. The study conducted by Inkinen et al. [23] present the most important analysis and characterization methods for quality assessment of PLA. Also, the simplified production routes of PLA and the most important properties of PLA were presented.

Since mechanical properties are important for printed parts, the influence of printing parameters on mechanical properties was studied to select the good settings. Most home users have no way of testing the strength of their parts and no extensive information is currently available about the mechanical properties of parts printed specifically on RepRaps. This work involves determining optimal printing parameters that provide the best mechanical performance of part fabricated using an open-source 3D printer based on fused deposition modelling (FDM) technology.

The present study is organized as follows. The experimental procedures are presented in Section 2. The central composite design (CCD) used to achieve the experiments is presented in Section 3. The main experimental data obtained on

PLA are given and discussed in Section 4. An empirical model for tensile strength and Young's modulus has been established using the analysis of variance (ANOVA). Finally, the major conclusions of the paper are summarized in Section 5.

2. Experimental procedures

2.1. *Fused Deposition Manufacturing (FDM)*

Fused Deposition Manufacturing (FDM) 3D printing is a process of manufacturing a three-dimensional object by laying down and fusing materials together in layers [3]. FDM technology is the most flexible, low cost, and a popular method of 3D printing today. Also, FDM allows to build 3D pieces of complex geometry. This technology uses heated thermoplastic filaments which are extruded from the tip of nozzle in a prescribed manner in a semi molten state and solidify at chamber temperature. A thermoplastic filament is wound on a reel which is unwound to supply material to an extrusion nozzle head. The nozzle head heats the material and turns the flow on and off. Typically stepper motors are used to move the extrusion head and adjust the flow. The head is moved in both horizontal x-axis and y-axis, while the build platform moves up and down (z-axis). The control of this mechanism is carried out using a computer-aided manufacturing (CAM) software tool which runs a microcontroller (Fig. 1). A heated nozzle deposits molten polymer onto a supportive structure layer by layer. Various polymers are used, including acrylonitrile butadiene styrene (ABS), polycarbonate (PC), poly-lactic acid (PLA).

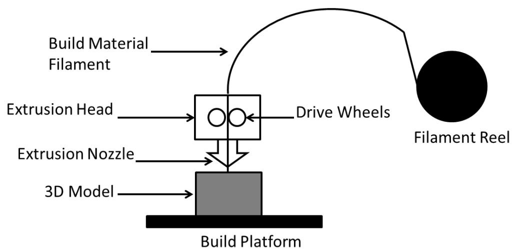

Figure 1 Illustration of the working principle of FDM-based 3D printing

2.2. *3D printer machine*

The 3D printer used to make the samples is WANHAO Duplicator 4S (see Fig. 2). It based on FDM technology. It has a build volume of 22.5 x 14.5 x 15 cm. It contains a dual extruder that prints ABS and PLA and other polymer filaments. After the creation of a 3D model by a computer-aided design (CAD) software, the file must be transformed into STL file format. Then, this file is transferred to the host software which converts them into G-code files which contains the instructions to obtain the final 3D objects. The WANHAO Duplicator 4S heats the PLA filament and squeezes it out through a nozzle of diameter 0.4 mm to make a solid object layer by layer. This method is called Fused Filament Fabrication [FFF].

Figure 2 The 3D printer WANHAO DUPLICATOR 4S

2.3. *Material*

The Poly-L-lactic Acid (PLA) wire used to produce the samples was provided with the WANHAO 3D printer. The diameter of this PLA filament is 1.75mm. It has a density of 1.25 g.cm^{-3}. The PLA has a melting temperature between 180°C-220°C and a glass transition temperature between 60-65°C [24]. The main physical and mechanical properties of several biopolymers (PLA, PC...) are presented in the study carried out by Van de Velde and Kiekens [24]. In a more detailed study by Farah et al. [25], the mechanical and physical properties affect the stability, degradation, aging and recyclability of PLA were studied. Also, the potential suitability of PLA to fulfill specific application requirements was discussed.

2.4. *Preparations of the Samples*

The tensile samples was created according to the standard EN ISO 527-2: 1996. The sample of the type 1BA is used (see Fig. 4). A .STL file of a tensile test sample was distributed online for anyone to print and send to the researchers for testing [26]. The .STL files were sliced into machine readable G-code. After, each sample was printed by modifying several settings including: deposition angle (A), extruder temperature (T) and printing speed (S). The other parameters remain constant such as infill (100 %), nozzle diameter (0.4 mm), cooling and layer height (0.2 mm). Three different deposition angles were studied: 0°, 30° and 60° as shown in Fig. 3. The printing speed is taken equal to 30 mm/s, 50 mm/s and 70 mm/s. Observation has shown that a 10 °C temperature change causes visible quality differences of a 3D print, which is assumed to change the mechanical properties as well. For the extruder temperature, three values were considered: 190°C, 200°C and 210°C.

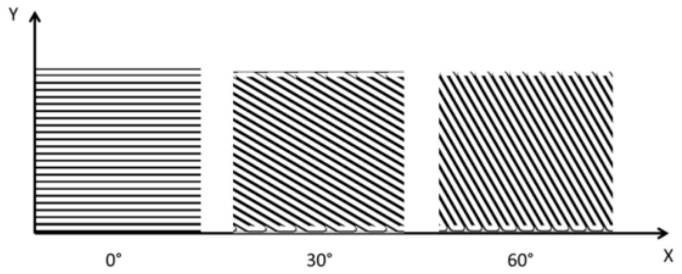

Figure 3 Deposition angles

2.5. *Tensile Testing*

The tensile tests were performed on an INSTRON 5569 machine at a fixed crosshead speed of 5 mm.min^{-1}. The specimens are printed into dumbbell shapes (type 1BA), according to the standard EN ISO 527-2 : 1996 (Plastics – Determination of tensile properties). Figure 4 shows the shape and dimensions of test specimen. The Young's modulus is calculated from the slope of the stress–strain curve. Three samples were tested for each combination of print settings using FDM WANHAO Duplicator 4S machine. All tests are carried out at the temperature 23±2 °C and relative humidity 50 ± 10% as per the standard EN ISO 527-2:1996. Here, the factors (Table 1) are set as per experiment plan (Table 2). The tensile strength and elastic modulus of 3D printed parts are measured by changing the printing parameters. It is noticed that three important printing parameters such as deposition angle (A), extruder temperature (T) and printing speed (S) influence the strength of printed parts by FDM technology. Many specimens broke outside of the gage length due to assumed stress concentrations in the regions changing geometry as was also seen by [27]. Data were included in this study for specimens that broke out of the gage length, but displayed a distinct maximum stress before failure. For this reason conclusions could be made only for modulus and maximum strength, not specimen failure or elongation.

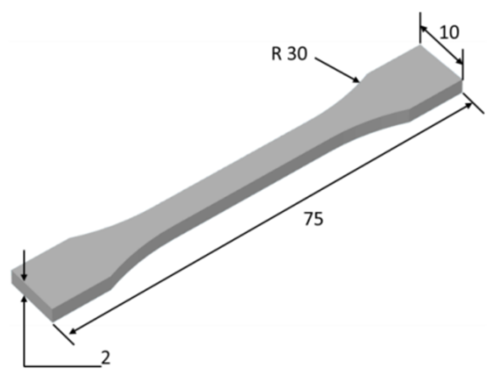

Figure 4 Tensile test specimen (Type 1BA), all dimensions are in mm

The central composite design (CCD) was used to achieve the experiments [28]. It is allow to establish an empirical model for tensile strength and Young's modulus. A half factorial design (K factors each at two levels) is considered to reduce the experiment run. Maximum and minimum value of each factor is coded into +1 and −1. Also, zero level (center point) and level (axial points) of each factor is also included. In this study, face centered central composite design (FCCCD) in which was used. This design locates the axial points on the centers of the faces of cube and requires only three levels for each factor. Three center points have been taken into consideration to get a reasonable estimate of experimental error. The factors and their levels are summarized in Tab. 1. Other factors are kept at their fixed level. Half factorial design having 8 experimental run, 6 ($2K$, where $K = 3$) axial run and 3 center run is shown in Tab. 2 together with the response value for tensile strength and Young's modulus.

Table 1 Factors and their level

Factor	Symbol	Unit	Low level (-1)	Centre point (0)	High level (+1)
deposition angle	A	Degree	0	30	60
extruder tempe.	T	°C	190	200	210
printing speed	S	mm/s	30	50	70

3. Experimental Plan

Table 2 Experimental data obtained from the FCCCD runs

Run order	Factor (coded units)			Tensile strength [MPa]	Young's modulus [MPa]
	A	T	S		
1	-1	-1	-1	19.4	3942.0
2	1	-1	-1	15.9	2494.1
3	-1	1	-1	19.3	3529.2
4	1	1	-1	16.3	2806.4
5	-1	-1	1	20.9	3714.4
6	1	-1	1	17.7	3147.8
7	-1	1	1	16.3	2568.2
8	1	1	1	15.8	2638.9
9	0	0	1	18.9	2963.3
10	0	0	-1	18.2	3327.5
11	0	1	0	17.4	3084.8
12	0	-1	0	23.6	2645.8
13	1	0	0	18.9	3704.1
14	-1	0	0	17.1	3485.6
15	0	0	0	19.2	3200.7
16	0	0	0	19.5	3250.5
17	0	0	0	19.7	3270.4

4. Results and Discussion

4.1. *Analysis of Experiments*

A full quadratic response surface model based on analysis of variance (ANOVA) was used to analyze the experimental data obtained from FCCCD. This model is therefore given explicitly by:

$$Y = B_0 + \sum_{i=1}^{i=k} B_i X_i + \sum_{i=1}^{i=k} B_{ii} X_i^2 + \sum_{i<j}\sum B_{ij} X_i X_j \, , \tag{1}$$

where Y is the response, X_i is ith factor, k is total number of factors.

Tables 3 and 4 summarize the ANOVA results for tensile strength and Young's modulus. For significance check, F value given in ANOVA table is used. Probability of F value greater than calculated F value due to noise is indicated by p value. For lack of fit, p value must be greater than 0.05. An insignificant lack of fit is desirable because it indicates any term left out of model is not significant and developed model fits well. It is noticed that the p-value is greater than 0.05 and lack of fit is more than 0.05 for this experiments. Also, it is reported that all the terms are significant for tensile strength and Young's modulus: linear, square and interaction terms.

The t-test was performed to determine the individual significant term at 95% of confidence level and final response surface equations for tensile strength T_s and Young's modulus E are given by equations (2) and (3), respectively, in terms of uncoded units. The coefficient of determination (R^2) is 73.4% and 78.7% for tensile strength and Young's modulus, respectively. This coefficient indicates the percentage of total variation in the response explained by the terms in the model. Also, it indicates that the model fits the data adequately.

$$\begin{aligned} T_s &= 19.54 - 0.836A - 1.233T + 0.076S - 1.611A^2 + 0.884T^2 - 1.092S^2 \\ &+0.405A \times T + 0.337A \times S - 0.857T \times S \end{aligned} \tag{2}$$

$$\begin{aligned} E &= 3245 - 244.8A - 131.7T - 106.7S + 347A^2 - 383T^2 - 103S^2 \\ &+170A \times T + 209A \times S - 194T \times S \end{aligned} \tag{3}$$

Table 3 ANOVA table for Tensile strength. DOF, degree of freedom; SS, sum of square; MS, mean sum of square

Source	**DOF**	**SS**	**MS**	**F-Value**	**p-Value**
Model	9	46.5024	5.1669	2.14	0.163
Linear	3	22.2502	7.4167	3.08	0.1
Square	3	16.1515	5.3838	2.24	0.172
2-Way Interaction	3	8.1007	2.7002	1.12	0.403
Lack of Fit	5	16.7354	3.3471	52.85	0.019
Pure Error	2	0.1267	0.0633		
Total	16	63.3644			

Table 4 ANOVA table for Young's modulus. DOF, degree of freedom; SS, sum of square; MS, mean sum of square

Source	**DOF**	**Adj SS**	**Adj MS**	**F-Value**	**P-Value**
Model	9	2366802	262978	2.88	0.089
Linear	3	886467	295489	3.23	0.091
Square	3	595573	198524	2.17	0.179
2-Way Interaction	3	884763	294921	3.23	0.091
Lack of Fit	5	637020	127404	98.84	0.07
Pure Error	2	2578	1289		
Total	16	3006401			

The normality test results are shown in Figs. 5 and 6 for tensile strength and Young's modulus, respectively. Since p-value of the normality plots is found to be above 0.05, it signifies that residue follows normal distribution. Once the models are validated, average relative error between the predicted value obtained by the model and experimental result shown in Tab. 2 are found to be 4.6% and 4% for tensile strength and Young's modulus, respectively. Small percentage of errors proves the suitability of above models for practical engineering applications.

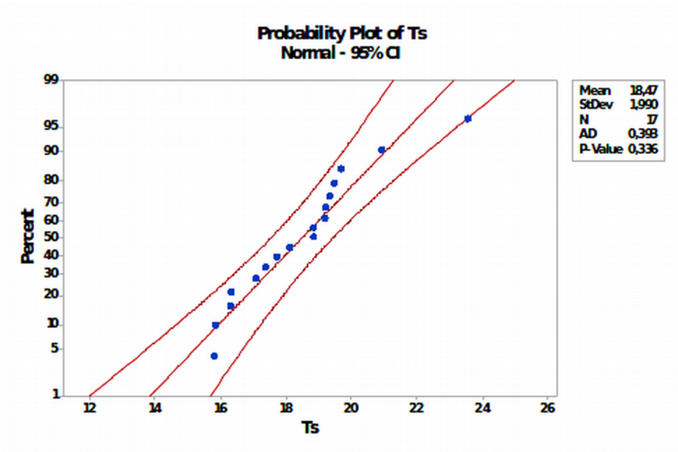

Figure 5 Normal probability plot of tensile strength at 95% of confidence interval

4.2. *Young's Modulus E and Tensile Strength T_s Determination*

Figure 7 shows a representative stress–strain curve of the studied material (PLA). Young's modulus E is measured during the tensile test according to the longitudinal direction of specimen. It is determined from the slope of the linear part of the stress–strain curve. On the other hand, tensile strength is the measure of the maximum stress that material can withstand without being elongated, stretched or pulled. The highest point of the stress-strain curve is the tensile strength. The obtained results are shown in Tab. 2 for Young's modulus E and tensile strength T_s.

The stress–strain curve indicates the brittle nature of failure. The staircase pattern shows that force per unit area has reached a value at which material continues

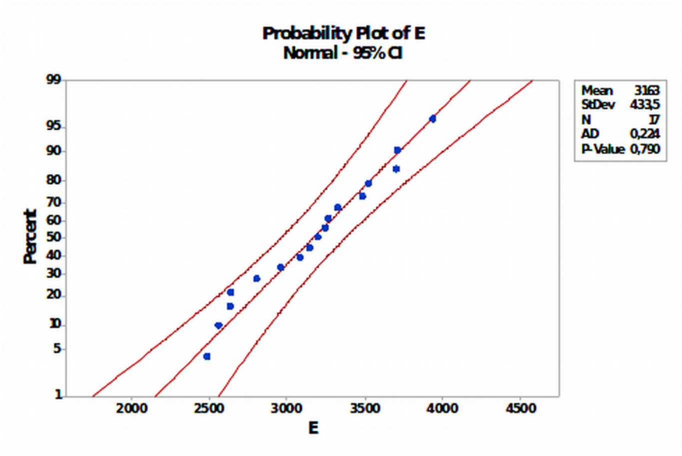

Figure 6 Normal probability plot of Young's modulus at 95% of confidence interval

to deform. After that it increases without causing significant deformation. This pattern is repeated in regular steps until the specimen fractures.

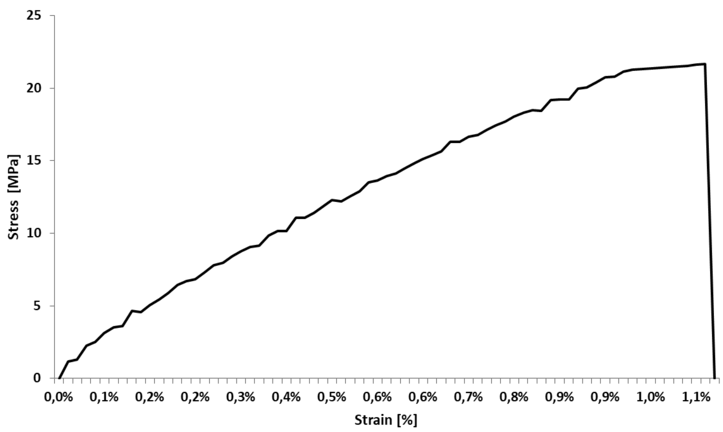

Figure 7 Experimental curve of the tensile test for PLA samples

4.3. *Optimization of Process Parameters*

Above discussion shows that FDM process involves large number of conflicting factors making it difficult to predict the mechanical properties based on simple analysis of factor variation. Hence, to determine the optimal setting of process parameters that will maximize the tensile strength and Young's modulus, desirability function

(DF) given by equation (4) is used.

$$DF = \left(\prod_{i=1}^{i=n} d_i^{w_i} \right)^{\frac{1}{\sum_{i=1}^{i=n} w_i}}, \tag{4}$$

where d_i is the desirability defined for the i-th targeted output; $w_i$is the weight. Since tensile strength and Young's modulus are equally important therefore value of weight w_ii is taken as 1. For a goal to find a maximum, d_i is calculated as shown in:

$$\begin{cases} d_i = 0 \quad \text{if} \quad Y_i \leq \text{Low}_i \\ d_i = \left[\frac{Y_i - \text{Low}_i}{\text{High}_i - \text{Low}_i} \right] \quad \text{if} \quad \text{Low}_i < Y_i < \text{High}_i \\ \text{d}_\text{i} = 1 \quad \text{if} \quad Y_i \geq \text{High}_i \end{cases} \tag{5}$$

where Y_i is the found value of the ith output during optimization process; the Low_i and High_i are the minimum and maximum values respectively of the experimental data for the i-th output.

Table 5 Optimum factor levels and predicted response for tensile strength and Young's modulus

Response	Goal	Low	High	w_i	Factor level (coded units)	Predicted response	DF
T_s	Max	15.8	23.6	1	A=-0.3535; T=-1; S=0.3737	22.04	0.8028
E	Maxi	2494	3942	1	A=-1; T=-0.1313; S=-1	4057	1

Optimum factor levels that will maximize the desirability function are calculated and are given in Tab. 5 for respective tensile strength and Young's modulus together with its predicted value. The combine desirability function when each response is maximized simultaneously together with optimum factor levels is given in Tab. 6.

Table 6 Optimum factor levels and predicted response for tensile strength and Young's modulus simultaneously

Response	Goal	Low	High	w_i	Factor level (coded units)	Predicted response	DF
T_s	Max	15.8	23.6	1	A=-1; T=-1; S=0.0303	21.3	0.783
E	Max	2494	3942	1		3752	

Optimum factor levels and predicted response for tensile strength and Young's modulus independently

5. Conclusions

The present study quantified the mechanical properties of printed components by open-source 3D printers for PLA material. A relationship between 3D printing parameters and mechanical properties of printed pieces were established using analysis of variance (ANOVA). The 3D printing parameters considered are deposition angle, extruder temperature and printing speed. On the other hand, the studied mechanical properties are tensile strength and Young's modulus. They are determined experimentally by tensile testing.

It has been found that the mechanical properties of the printed parts strongly depend on the printing process parameters. The effect of various factors or parameters and their interactions can be observed but difficult to assign exact reasons. The interactions between the parameters play an important role. Indeed, Part build mechanism in FDM is a complex phenomenon. The optimal factor levels were evaluated using the desirability function concept. The proper adjustments improve significantly the tensile strength and Young's modulus independently and simultaneously. The factor levels of simultaneous optimization are different from individual optimal factor setting. Also, the normality test shows that error between the predicted values and experimental values is normally distributed, with very small percentage of error between the predicted and experimental values.

Acknowledgements

The authors thank Prof. Ali Nourdine from Savoie Mont-Blanc University – France, for their help and the supply of the experimental device.

References

[1] **Mansour, S. and Hague, R.**: Impact of rapid manufacturing on design for manufacture for injection moulding, *Proceedings of the Institution of Mechanical Engineers, Part B: Journal of Engineering Manufacture*, **217**(4), 453–461, **2003**.

[2] **Goyanes, A., Wang, J., Buanz, A., Martínez-Pacheco, R., Telford, R., Gaisford, S. and Basit, A.W.**: 3D printing of medicines: engineering novel oral devices with unique design and drug release characteristics, *Molecular Pharmaceutics*, **12**(11), 4077–4084, **2015**.

[3] **Dimitrov, D., Schreve, K. and De Beer, N.**: Advances in three dimensional printing-state of the art and future perspectives, *Rapid Prototyping Journal*, **12**(3), 136–147, **2006**.

[4] **Kruth, J.-P., Levy, G., Klocke, F. and Childs, T.**: Consolidation phenomena in laser and powder-bed based layered manufacturing, *CIRP Annals-Manufacturing Technology*, **56**(2), 730–759, **2007**.

[5] **Melchels, F.P., Feijen, J. and Grijpma, D.W.**: A poly (D, L-lactide) resin for the preparation of tissue engineering scaffolds by stereolithography, *Biomaterials*, **30**(23), 3801–3809, **2009**.

[6] **Ford, S. and Despeisse, M.**: Additive manufacturing and sustainability: an exploratory study of the advantages and challenges, *Journal of Cleaner Production*, **137**, 1573–1587, **2016**.

[7] **Jones, R., Haufe, P., Sells, E., Iravani, P., Olliver, V., Palmer, C. and Bowyer, A.**: RepRap – the replicating rapid prototyper, *Robotica*, **29**(1), 177–191, **2011**.

[8] **Pearce, J.M.**: *Open-source lab: how to build your own hardware and reduce research costs*, Newnes, **2013**.

[9] **Sugavaneswaran, M. and Arumaikkannu, G.**: Modelling for randomly oriented multi material additive manufacturing component and its fabrication, *Materials & Design*, **54**, 779–785, **2014**.

[10] **Drumright, R.E., Gruber, P.R. and Henton, D.E.**: Polylactic acid technology, *Advanced Materials*, **12**(23), 1841–1846, **2000**.

[11] **Carothers, W.H., Dorough, G.L. and Natta, F.J.V.**: Studies of Polymerization and Ring Formation. X. the Reversible Polymerization of Six-Membered Cyclic Esters, *Journal of the American Chemical Society*, **54**(2), 761–772, **1932**.

[12] **Lasprilla, A.J., Martinez, G.A., Lunelli, B.H., Jardini, A.L. and Maciel Filho, R.**: Poly-lactic acid synthesis for application in biomedical devices – A review, *Biotechnology Advances*, **30**(1), 321–328, **2012**.

[13] **Scaffaro, R., Lopresti, F., Botta, L., Rigogliuso, S. and Ghersi, G.**: Preparation of three-layered porous PLA/PEG scaffold: relationship between morphology, mechanical behavior and cell permeability, *Journal of the Mechanical Behavior of Biomedical Materials*, **54**, 8–20, **2016**.

[14] **Montjovent, M.-O., Mark, S., Mathieu, L., Scaletta, C., Scherberich, A., Delabarde, C., Zambelli, P.-Y., Bourban, P.-E., Applegate, L. A. and Pioletti, D. P.**: Human fetal bone cells associated with ceramic reinforced PLA scaffolds for tissue engineering, *Bone*, **42**(3), 554–564, **2008**.

[15] **Arrieta, M. P., López, J., Hernández, A. and Rayón, E.**: Ternary PLA–PHB–Limonene blends intended for biodegradable food packaging applications, *European Polymer Journal*, **50**, 255–270, **2014**.

[16] **Wang, L.-F., Rhim, J.-W. and Hong, S.-I.**: Preparation of poly(lactide)/poly(butylene adipate-co-terephthalate) blend films using a solvent casting method and their food packaging application, *LWT - Food Science and Technology*, **68**, 454–461, **2016**.

[17] **Murariu, M. and Dubois, P.**: PLA composites: From production to properties, *Advanced Drug Delivery Reviews*, **107**, 17–46, **2016**.

[18] **Heidari, B.S., Oliaei, E., Shayesteh, H., Davachi, S.M., Hejazi, I., Seyfi, J., Bahrami, M. and Rashedi, H.**: Simulation of mechanical behavior and optimization of simulated injection molding process for PLA based antibacterial composite and nanocomposite bone screws using central composite design, *Journal of the Mechanical Behavior of Biomedical Materials*, **65**, 160–176, **2017**.

[19] **Lu, L., Peter, S.J., Lyman, M.D., Lai, H.-L., Leite, S.M., Tamada, J.A., Uyama, S., Vacanti, J.P., Langer, R. and Mikos, A.G.**: In vitro and in vivo degradation of porous poly (DL-lactic-co-glycolic acid) foams, *Biomaterials*, **21**(18), 1837–1845, **2000**.

[20] **Singh, S., Ramakrishna, S. and Singh, R.**: Material issues in additive manufacturing: A review, *Journal of Manufacturing Processes*, **25**, 185–200, **2017**.

[21] **Hamad, K., Kaseem, M., Yang, H., Deri, F. and Ko, Y.**: Properties and medical applications of polylactic acid: A review, *Express Polymer Letters*, **9**(5), 435–455, **2015**.

[22] **Olivieri, R., Di Maio, L., Scarfato, P. and Incarnato, L.**: Preparation and characterization of biodegradable PLA/organosilylated clay nanocomposites, in: *VIII International Conference on "Times of Polymers and Composites": From Aerospace to Nanotechnology*, 020102, **2016**.

[23] **Inkinen, S., Hakkarainen, M., Albertsson, A.-C. and Sodergard, A.**: From lactic acid to poly (lactic acid)(PLA): characterization and analysis of PLA and its precursors, *Biomacromolecules*, **12**(3), 523–532, **2011**.

[24] **Van de Velde, K. and Kiekens, P.**: Biopolymers: overview of several properties and consequences on their applications, *Polymer Testing*, **21**(4), 433–442, **2002**.

[25] **Farah, S., Anderson, D. G. and Langer, R.**: Physical and mechanical properties of PLA, and their functions in widespread applications — A comprehensive review, *Advanced Drug Delivery Reviews*, **107**, 367–392, **2016**.

[26] EN ISO 527-2: **1996** Test specimens for determination of tensile properties. http://www.thingiverse.com/thing:190386.

[27] **Ahn, S.-H., Montero, M., Odell, D., Roundy, S. and Wright, P. K.**: Anisotropic material properties of fused deposition modeling ABS, *Rapid Prototyping Journal*, **8**(4), 248–257, **2002**.

[28] **Montgomery, D.C.**: *Design and analysis of experiments*, John Wiley & Sons, **2017**.